

Submicron hybrid vesicles consisting of polymer-lipid and polymer-cholesterol blends

Svenja Winzen,^a Max Bernhardt,^a David Schaeffel,^a Amelie Koch,^a Michael Kappl,^a Kaloian Koynov,^a Katharina Landfester^a and Anja Kroeger^{*a}

^a *Max Planck Institute for Polymer Research, Ackermannweg 10, 55128 Mainz, Germany.*

ELECTRONIC SUPPLEMENTARY INFORMATION

Synthesis of Alexa-Fluor 647[®] – PDMS-*b*-PMOXA

Initially 100 µg of Alexa Fluor 647[®] succinimidyl ester were weighed into a brown-glass vial and immediately dissolved in 25 µL dry DMSO and subsequently 185 µL of a solution of PDMS-*b*-PMOXA (2.5 g/L in dry ethanol) were added. The vial was flushed with helium and stirred overnight (500 U/min). Afterwards 350 µL of dry ethanol were added to dilute the solution to a concentration of $c = 1$ g/L. The resulting stock solution was used for the preparation of vesicles without any further purification.

Vesicle preparation

For the preparation of polymersomes 5 mg of PDMS-*b*-PMOXA were dissolved in 5 mL of chloroform in a 10 mL round bottom flask by shaking for 1 h. Afterwards the chloroform was removed under reduced pressure. The remaining film was dried in a vacuum oven for 1 h. Rehydration was done by adding 5 mL of water afterwards. The solution was stirred on a magnetic stirring plate overnight (500 U/min). The resulting multilamellar vesicles were extruded with a LiposoFast-Basic-Extruder (Avestin, Canada) 11 times through polycarbonate membranes (Avestin, Canada) with pore sizes of 800 nm followed by 400 nm and 200 nm to homogenize the final vesicle size of $R_h \sim 110$ nm.

Liposomes were prepared according to the procedure for polymersomes. Prior to extrusion the solutions were sonicated for 20 min at 50 °C in a Sonorex Super RK 514H bath sonicator (Bandelin, Germany).

The preparation procedure of polymersomes (see above) was also used for the formation of hybrid vesicles. Lipid-block-copolymer-vesicles were formed in molar ratios of 90:10 and 50:50 (block-copolymer : lipid) and cholesterol-block-copolymer-vesicles in molar ratios of 95:5 and 50:50 (block-copolymer : cholesterol). The components were mixed prior to dissolution in chloroform.

For fluorescently labelled vesicles 1 mol% of the initial block-copolymer was replaced by Alexa Fluor 647[®] – PDMS-*b*-PMOXA. A fraction of 10 mol% of DMPC was replaced by Bodipy[®] 500/510 C₁₂-HPC according to the mixing ratio 90:10. For cholesterol 10 mol% of TopFluor[®] cholesterol were

added according to the mixing ratio 95:5.

Details on light scattering experiments

All measurements were carried out at temperature $T = 20$ °C. Dust-free solutions were obtained by filtration through mixed cellulose ester membrane filters with a pore size of 0.45 μm (Millipore, Millex-HA) for samples with $c = 1$ g/L and through PVDF membrane filters with a pore size of 5 μm (Millipore, Millex-SV) for samples with $c = 0.05$ g/L. The solutions were filtered into silica glass light scattering cuvettes (Hellma, inner diameter 18 mm), which were cleaned before with acetone in a Thurmont-apparatus. The refractive index increments of DMPC liposomes and PDMS-*b*-PMOXA polymersomes were determined at room temperature using a scanning Michelson interferometer at a wavelength of $\lambda = 633$ nm.

DLS data evaluation was performed by using the stretched exponential Kohlrausch-Williams-Watts (KWW) function¹ as well as the CONTIN algorithm^{2,3}. The KWW method assumes that for single but nonexponential decay, the computed relaxation function $C(q, t)$ can be represented by

$$C(q, t) = \exp[-(t/\tau \cdot (q))^\beta] \quad (1)$$

where τ is the relaxation time and β_{KWW} is the shape parameter ranging as $0 \leq \beta \leq 1$ characterizing the distribution of relaxation times. The CONTIN algorithm is used for the analysis of multiple decay processes and is given by

$$C(q, t) = \int_{-\infty}^{\infty} H_\tau(\ln \tau) \exp\left[-\frac{t}{\tau}\right] d(\ln \tau) \quad (2)$$

where $H_\tau(\ln \tau)$ is the distribution function of relaxation times.

Theoretical details on dual-color fluorescence cross-correlation spectroscopy

Fluorescence intensity fluctuations resulting from the diffusion of species containing fluorescently labelled lipids or block-copolymers through the confocal observation volume were detected separately in the respective detection channels and examined by means of the autocorrelation function $G(\tau) = \langle F(t)F(t + \tau) \rangle / \langle F(t) \rangle^2$ where $F(t)$ represents the fluorescent intensity. As shown theoretically⁴ for an ensemble of identical freely diffusing fluorescence species, $G(t)$ can be analytically described by:

$$G(\tau) = 1 + \frac{1}{N} \frac{1}{\left[1 + \frac{\tau}{\tau_D}\right] \sqrt{1 + \frac{\tau}{S^2 \tau_D}}} \quad (3)$$

Here, N is the number of diffusing fluorescence species in the observation volume V , τ_D is the diffusion time of the species and S is the so-called structural parameter representing the axial to radial ratio of the observation volume. The diffusion coefficient of the species D is related to τ_D by $D =$

$(r_0^2 + R_h^2)/4\tau_D$, where R_h is the hydrodynamic radius. Thus, by knowing the size and shape of the observation volume from reference measurements using fluorescent tracers with known diffusion coefficients (we used Alexa Fluor 488[®] and Alexa Fluor 647[®], purchased by life technologies) the concentration of the fluorescent species $c = N/V$, and their hydrodynamic radius R_h are accessible by equation 3.

An extension of the classical fluorescence correlation spectroscopy (FCS), so called dual-color fluorescence cross-correlation spectroscopy (DC-FCCS) was used to prove the existence and quantity of lipid-copolymer and cholesterol-copolymer hybrid vesicles. The principle is described in detail elsewhere.⁵ Briefly, the beams of the two different wavelength lasers mentioned above were made collinear and simultaneously focused into the sample by the microscope objective to create two overlapping observation volumes. The collected fluorescent light was separated by a dichroic mirror in a “block-copolymer” and “lipid/cholesterol” detection channel. As long as the two types of fluorescent species (block-copolymer and lipid/cholesterol) are diffusing independently through the observation volumes the temporal fluorescence fluctuations measured in the two detection channels will not be correlated. However, if these fluorescent species are linked, e.g. in a double-colored vesicle the fluorescence fluctuations will be strongly correlated. This is mathematically expressed in terms of a cross-correlation function $G_{cc}(\tau) = \langle F_1(t)F_2(t + \tau) \rangle / \langle F_1(t) \rangle \langle F_2(t) \rangle$ where the subscripts denote the two independent detection channels. The amplitude of this function $G_{cc}(0)$ is directly proportional to the concentration of the double-labeled species.⁶

Cryo-TEM sample preparation

For sample preparation 5 μL of the sample ($c = 0.2 \text{ g/L}$) were dropped onto a copper grid (Quantifoil R 2/2 Cu 300 mesh, Quantifoil Micro Tools, Germany). Excess liquid was removed with a filter paper and the grid was subsequently blotted with a vitrobot[™] system (FEI, USA). The sample was frozen in liquid ethane at $T = -178 \text{ }^\circ\text{C}$ and transferred to the TEM instrument. Statistical analyses of the membrane thicknesses were performed using ImageJ 1.45s software. All determined values are number averages of 100 measured items of different vesicles.

Details on atomic force microscopy measurements

40 μL of each vesicle solution ($c = 0.1 \text{ g/L}$) were placed on the freshly cleaved mica at the bottom of a small petri dish and left in a highly humid environment for 2 h, to let the vesicles adsorb on the surface. After floating the petri dish with Milli-Q water, imaging was carried out in the QI-mode, which generates a topographical image by taking a force-distance curve in each data point. Typically images with 128x128 data points and a scan size of 2.5 μm were acquired. Sample topography and height profiles were directly extracted by the JPKSPM data processing program from JPK instruments. We found that vesicles could be imaged more stably using QI mode compared to AC (intermittent contact) mode. After QI-imaging, force-distance curves were recorded on the top of a vesicle in force

spectroscopy mode. Mechanical properties of vesicles were extracted both from specific force curves within the QI data sets (i.e. those taken close to the top of the vesicles) and from force distance curves recorded in force spectroscopy mode. Data analysis yielded similar results for both methods, thus no distinction is made in the following. To convert the force versus distance curves taken on top of the vesicles to force versus indentation curves, reference force curves were recorded on the hard mica substrate to calibrate the deflection sensitivity of the AFM cantilevers. After subtracting the voltage offset obtained from fitting the zero force baseline, the deflection voltage signal of each curve is converted to force by dividing it by the deflection sensitivity and multiplying it with the spring constant of the cantilever. The distance is obtained by subtracting the cantilever deflection from the piezo position.⁷ To extract the mechanical properties of the vesicle membranes, we applied the thin shell theory⁸ as described in detail previously.⁹ Essentially, it relates the stiffness k_{mem} of the vesicle membrane, i.e. the slope of the observed linear force versus deformation curve, to the Young's modulus E of the shell material by:

$$k_{mem} = \frac{4Eh^2}{R\sqrt{3(1-\nu^2)}} \quad (4)$$

where ν is the Poisson ratio. The radius of curvature R of the vesicle that forms a spherical cap can be determined from its width W and height H as determined from the AFM image by simple geometric considerations:

$$R = \frac{0.25W^2 + H^2}{2H} \quad (5)$$

The bending modulus for a membrane with thickness h made of a material with Young's modulus E and Poisson ratio ν is given by:¹⁰

$$k_{bend} = \frac{Eh^3}{12(1-\nu^2)} \quad (6)$$

For the calculations, we used the membrane thickness values obtained from *cryo*-TEM imaging and assumed a value of 0.5 for the Poisson ratio ν .¹¹

Additional figures:

$^1\text{H-NMR}$:

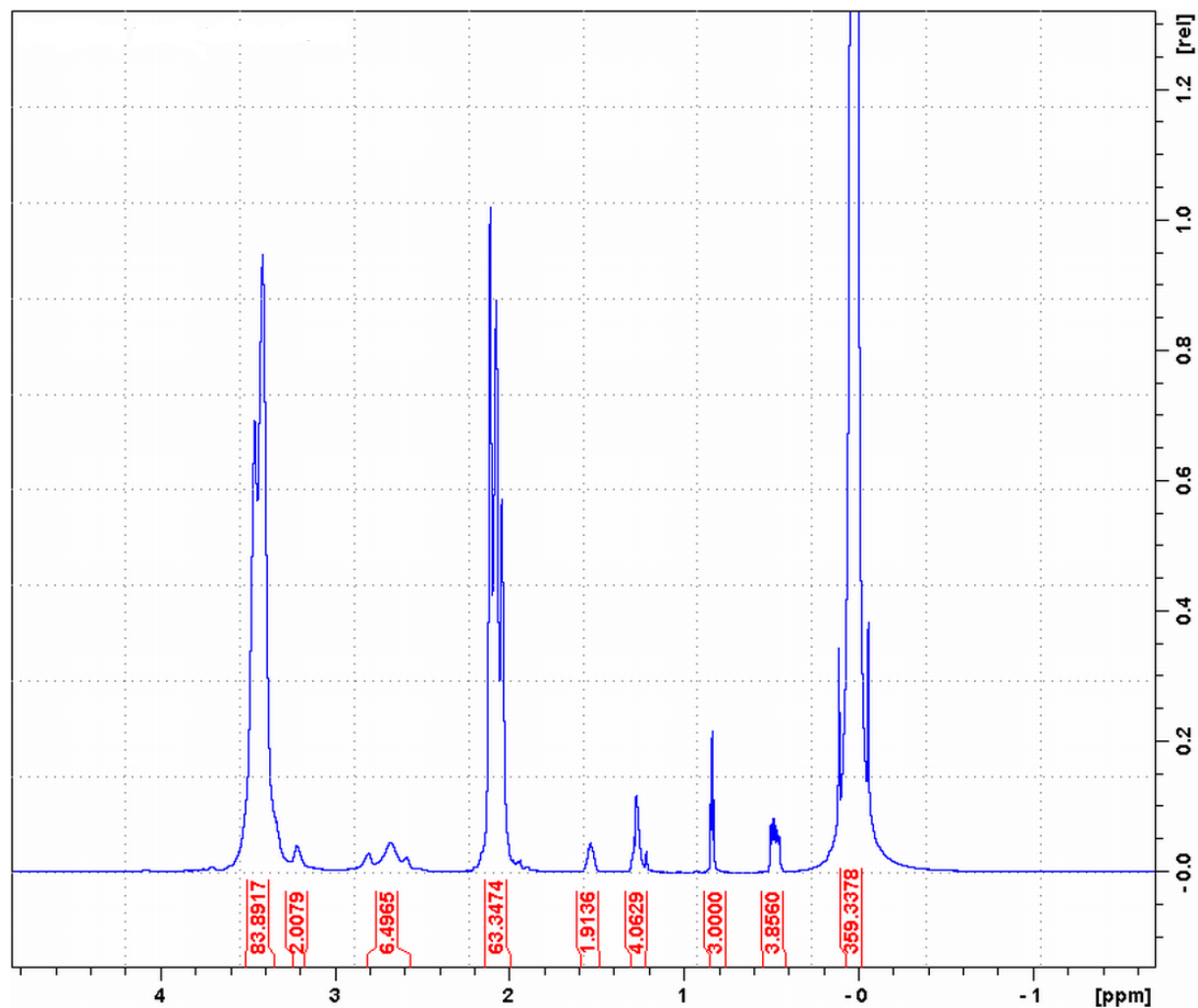


Fig. S1 $^1\text{H-NMR}$ spectrum of the diblock-copolymer $\text{PDMS}_n\text{-}b\text{-PMOXA}_m$ in CDCl_3 . The corresponding block lengths were determined to be $n = 60$ and $m = 21$.

$\delta\text{H/ppm}$ (700.1 MHz; CDCl_3) = -0.06-0.11 (6 H, br m, $\text{Si}(\text{Me})_2$), 0.48 (4 H, m, CH_2), 0.84 (3 H, t, Me), 1.27 (4 H, m, CH_2CH_2), 1.53 (2 H, m, CH_2), 2.07 (3 H, br m, COMe), 2.59-3.22 (8 H, br m, CH_2) and 3.44 (4 H, br m, CH_2CH_2).

Light scattering experiments:

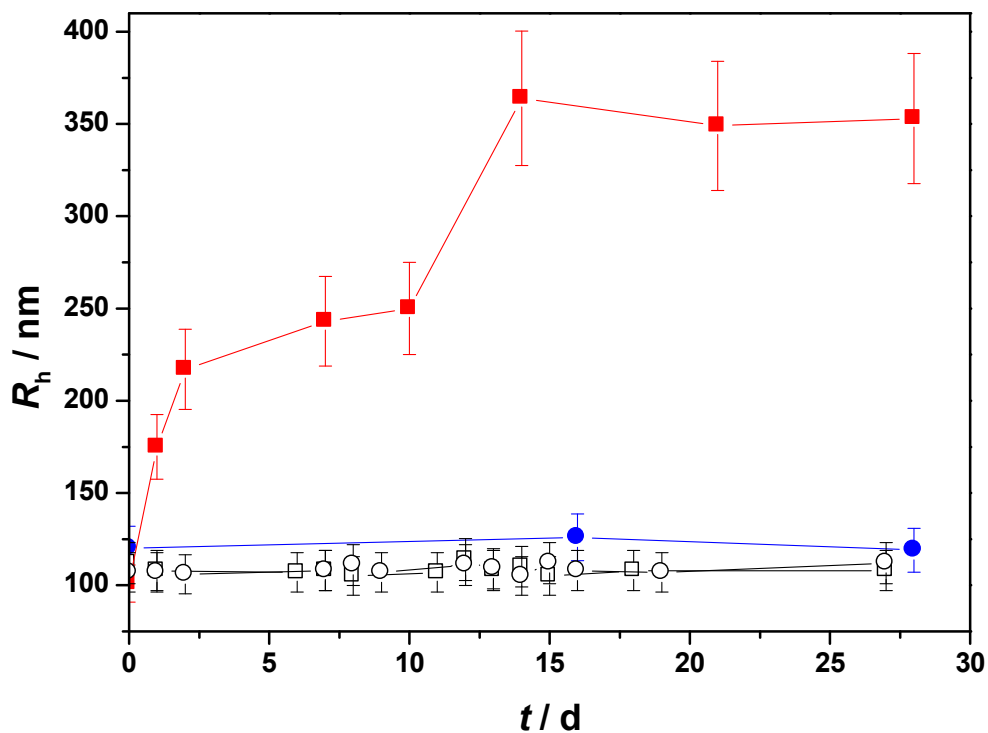


Fig. S2 Long term stability of BCP/DMPC vesicles with different DMPC fractions (BCP/DMPC 90/10 (□) and BCP/DMPC 50/50 (○)) compared to pure PDMS-*b*-PMOXA polymersomes (●) and pure DMPC liposomes (■).

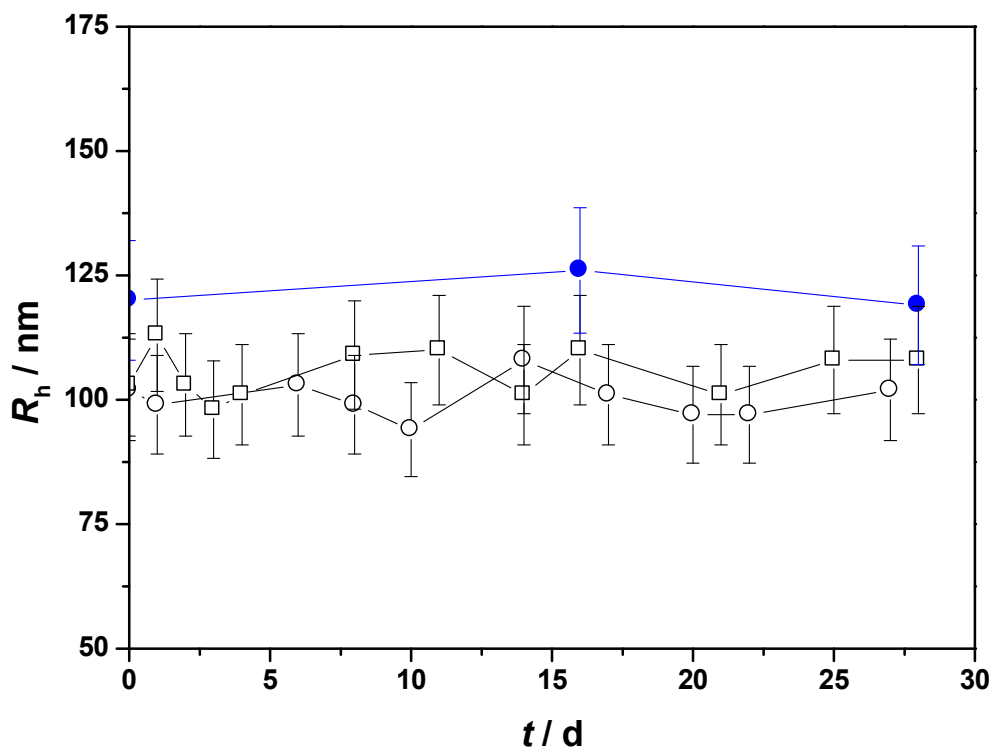


Fig. S3 Long term stability of BCP/Chol vesicles with different cholesterol fractions (BCP/Chol 95/5 (○) and BCP/Chol 50/50 (□)) compared to pure PDMS-*b*-PMOXA polymersomes (●).

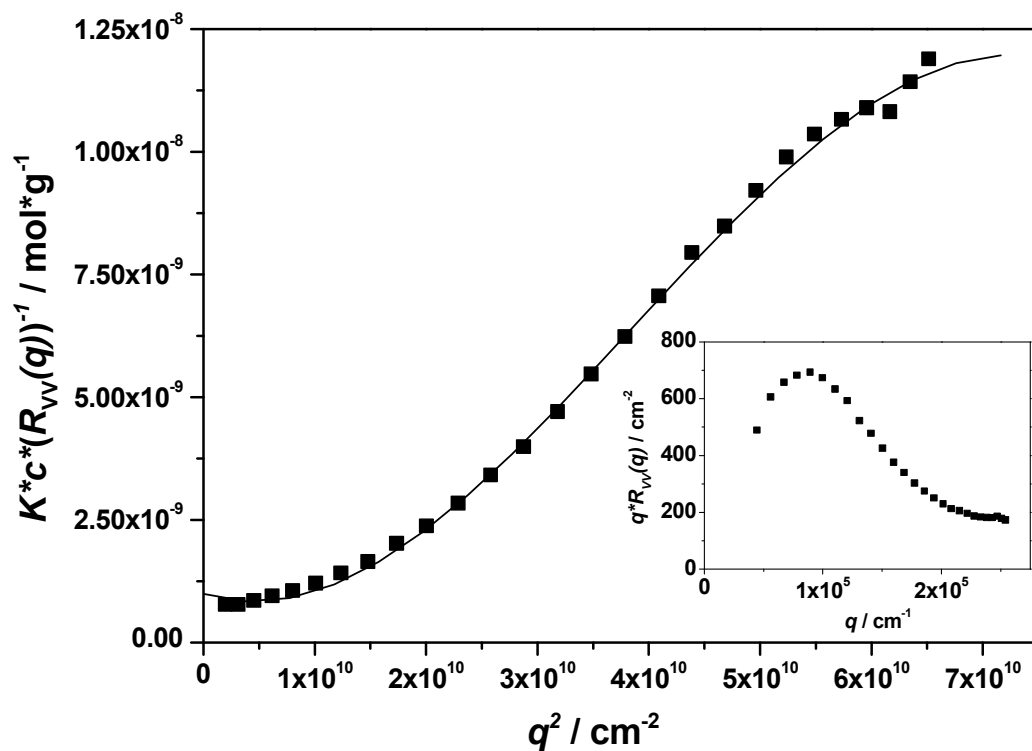


Fig. S4 Ornstein-Zernicke representation of the scattering data obtained from the total scattering intensities of PDMS-*b*-PMOXA polymersomes as a function of the scattering vector q^2 . The straight line represents a fit according to a cubic polynomial where the intercept gave the inverse of the apparent molecular weight M_{app} . **Inset:** Holtzer representation of the scattering data, where the q -value with the highest scattering intensity gave the inverse of the radius of gyration R_G .

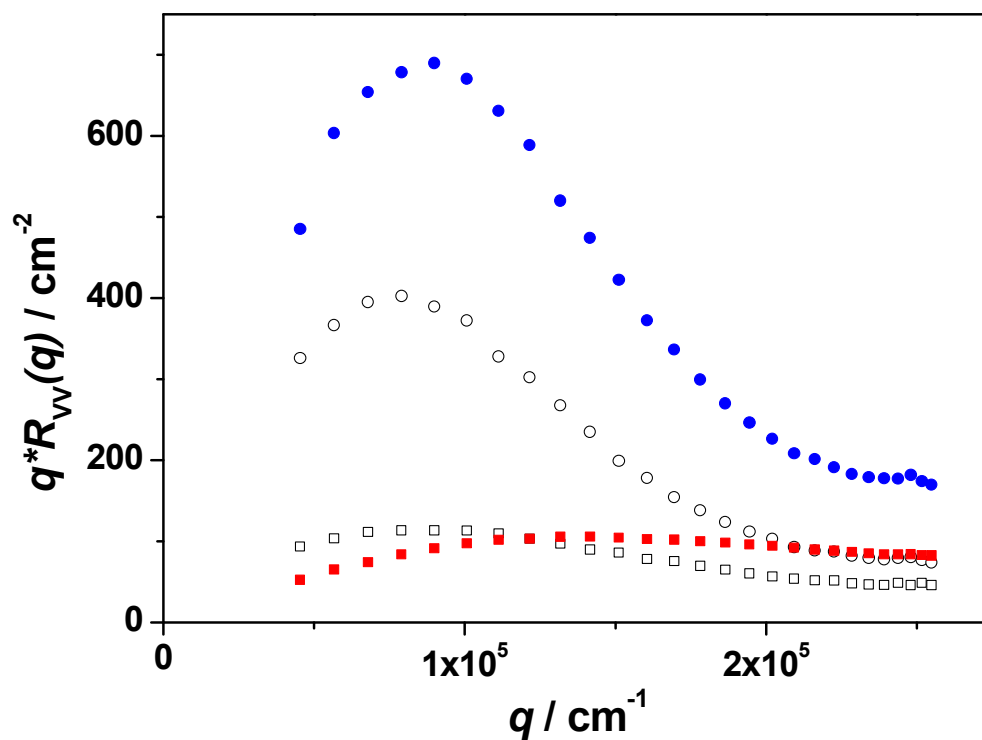


Fig. S5 Holtzer representation of the scattering data obtained from the total light scattering intensities as a function of the scattering vector q for PDMS-*b*-PMOXA polymersomes (●), DMPC liposomes (■), BCP/DMPC 90/10 (□) and BCP/DMPC 50/50 (○).

Cryo-TEM Imaging:

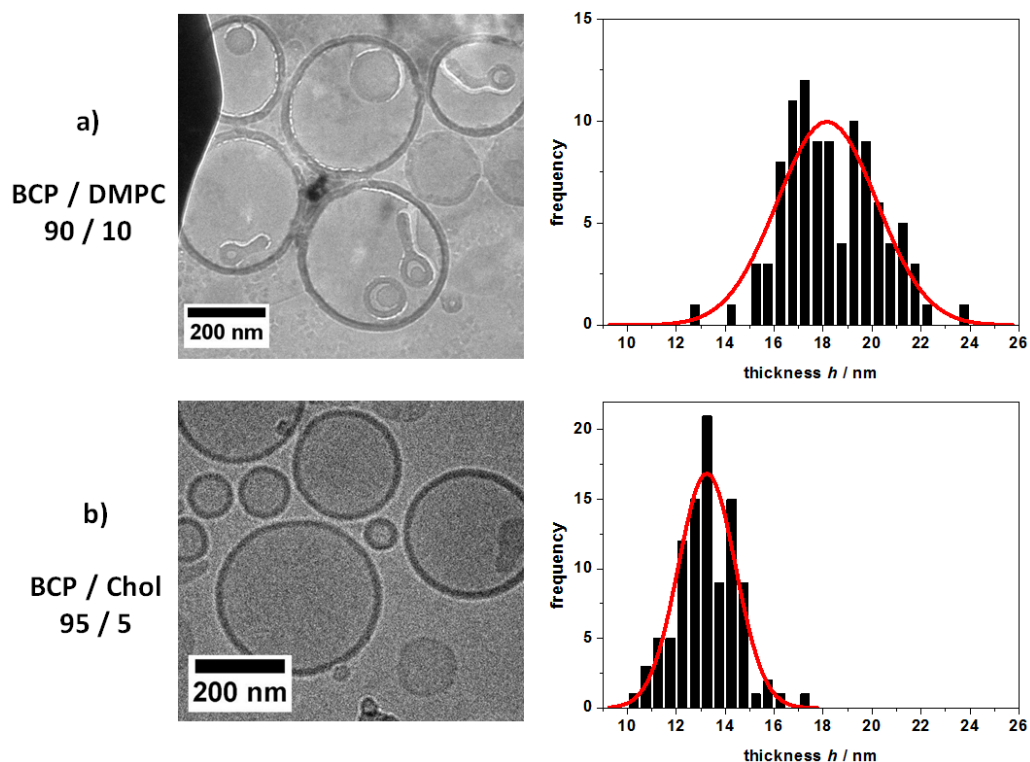


Fig. S6 Cryo-TEM images with corresponding histograms of measured membrane thicknesses containing a Gaussian fit. a) Hybrid vesicles containing 90 mol% BCP and 10 mol% DMPC. b) Hybrid vesicles containing 95 mol% BCP and 5 mol% Chol.

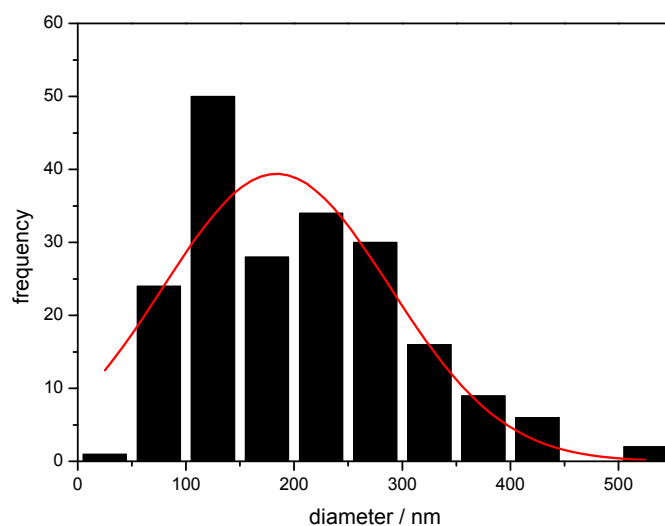


Fig. S7 Histogram showing the diameter distribution of hybrid vesicles containing 90 mol% BCP and 10 mol% DMPC measured at 200 items of a series of cryo-TEM micrographs.

AFM Force measurements:

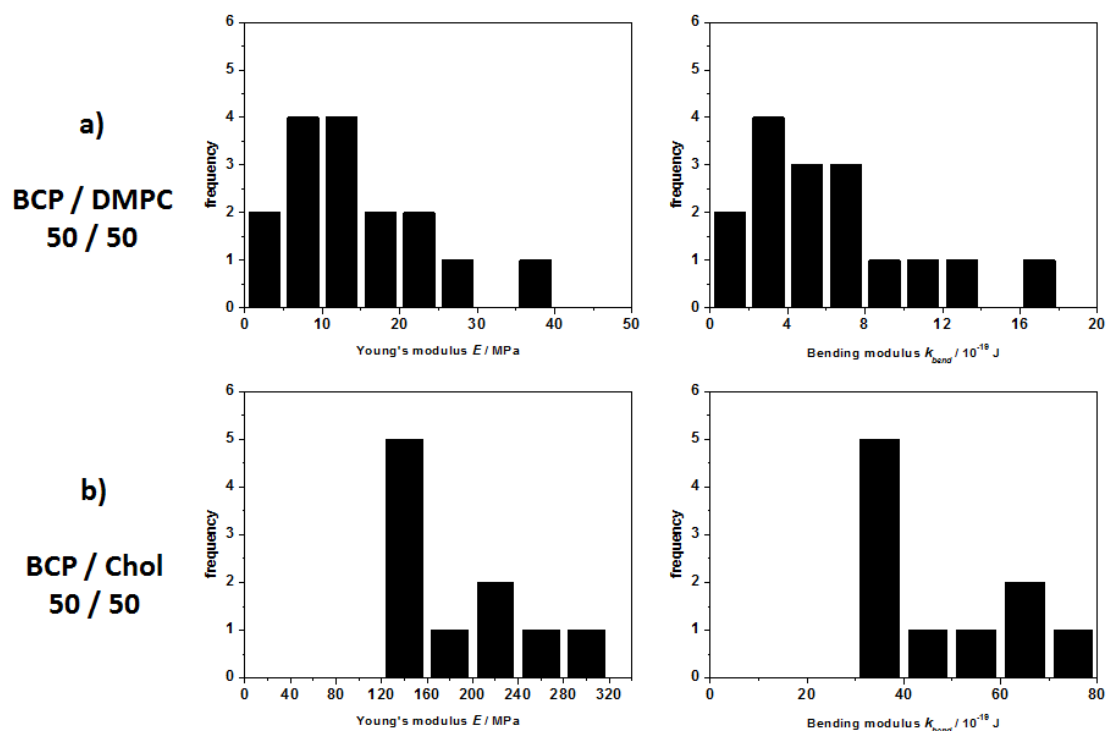


Fig. S8 Histograms of Young's and bending moduli determined from force-distance measurements for a) BCP/DMPC 50/50 vesicles and b) BCP/Chol 50/50 vesicles. For BCP/DMPC 50/50 a total of 16 vesicles and for BCP/Chol 50/50 a total of 10 vesicles were analyzed.

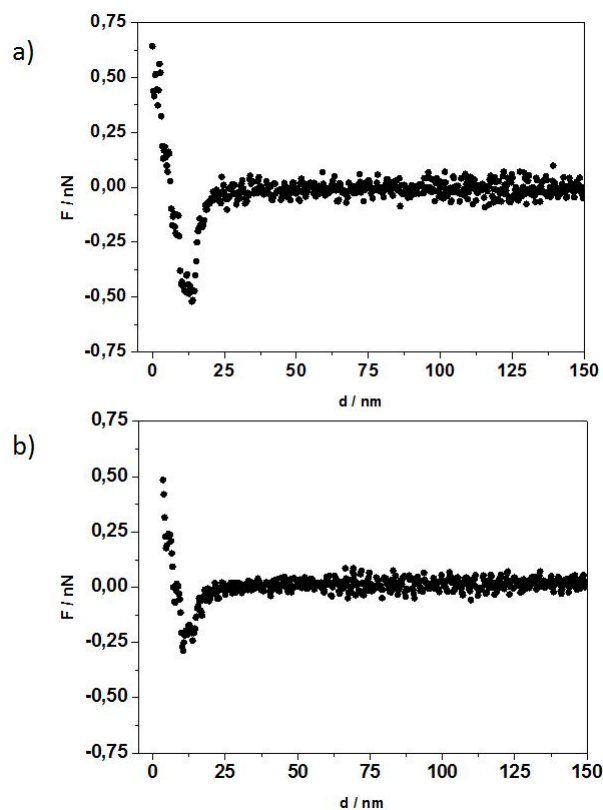


Fig. S9 Exemplary force-distance curves on a) muscovite mica and b) BCP/Chol hybrid vesicles which were used for the calculation of Young's and bending modulus

Additional references

1. W. Brown (Ed.), *Light scattering: Principles and Development*, Clarendon Press, Oxford, 1996.
2. S. W. Provencher, *Makromol. Chem.*, 1979, 180, 201-209.
3. S. W. Provencher, *Comput. Phys. Commun.*, 1982, 27, 229-242.
4. R. Rigler and E. Elson, *Fluorescence correlation spectroscopy : theory and applications*, Springer, Berlin; New York, 2001.
5. P. Schwille, F. J. MeyerAlmes and R. Rigler, *Biophys. J.*, 1997, 72, 1878-1886.
6. D. Schaeffel, R. H. Staff, H.-J. Butt, K. Landfester, D. Crespy and K. Koynov, *Nano Lett.*, 2012, 12, 6012-6017.
7. H.-J. Butt, B. Cappella and M. Kappl, *Surf. Sci. Rep.*, 2005, 59, 1-152.
8. E. Reissner, *J. Math. Phys.*, 1946, 25, 80-85.
9. K. Jaskiewicz, M. M. Makowski, M. Kappl, K. Landfester and A. Kroeger, *Langmuir*, 2012, 28, 12629-12636.
10. E. A. Evans, *Biophys. J.*, 1974, 14, 923-931.
11. N. Delorme and A. Fery, *Phys. Rev. E: Stat., Nonlinear, Soft Matter Phys.*, 2006, 74, 030901.